Substrate-Induced Symmetry Breaking in Silicene

Chun-Liang Lin,[1] Ryuichi Arafune,[2] Kazuaki Kawahara,[1] Mao Kanno,[3] Noriyuki Tsukahara,[1] Emi Minamitani,[4] Yousoo Kim,[4] Maki Kawai,[1,3] and Noriaki Takagi[1,3,*]

[1]*Department of Advanced Materials Science, Graduate School of Frontier Science, The University of Tokyo, Kashiwa 5-1-5, Chiba 277-8561, Japan*

[2]*International Center for Materials Nanoarchitectonics (WPI-MANA), National Institute for Materials Science, 1-1 Namiki, Ibaraki 304-0044, Japan*

[3]*Department of Applied Chemistry, The University of Tokyo, Hongo 7-3-1, Tokyo 113-8656, Japan*

[4]*RIKEN, 2-1 Hirosawa, Saitama 351-0198, Japan*

(Received 3 October 2012; published 11 February 2013)

We demonstrate that silicene, a 2D honeycomb lattice consisting of Si atoms, loses its Dirac fermion characteristics due to substrate-induced symmetry breaking when synthesized on the Ag(111) surface. No Landau level sequences appear in the tunneling spectra under a magnetic field, and density functional theory calculations show that the band structure is drastically modified by the hybridization between the Si and Ag atoms. This is the first direct example demonstrating the lack of Dirac fermions in a single layer honeycomb lattice due to significant symmetry breaking.

DOI: 10.1103/PhysRevLett.110.076801 PACS numbers: 73.22.−f, 61.46.−w, 68.37.Ef, 81.05.Zx

Honeycomb (HC) lattice materials such as graphene, MgB_2, and some organic conductors attract much attention because of their novel electronic properties [1–6], and silicene has recently joined the group of two-dimensional (2D) HC lattice materials. Density functional theory (DFT) calculations have revealed the geometric and electronic structures of freestanding silicene [7–11]. The freestanding silicene is stable in a lightly buckled structure in which the neighboring Si atoms are displaced alternatively perpendicular to the plane [7–11]. The electronic π- and π^*- bands derived from the Si $3p_z$ orbital disperse linearly to cross at the Fermi level (E_F), and the electrons behave as massless Dirac fermions reflecting the symmetry derived from the equivalence of between the two sublattices [9–14]. In addition, silicene has advantages over graphene: Silicene is a promising candidate for quantum spin Hall effects [10,15,16] and is more compatible with current Si-based device technologies.

To fabricate electronics devices, silicene is placed on solid substrates and its electronic properties are perturbed by interfacial couplings. Thus, it is crucial to unveil how the interfacial couplings affect both geometric and electronic structures. In particular, coupling may break the symmetry to drastically alter the electronic structure such as the energy gap at E_F. This may also open up key technologies to engineer the electronic properties by fine-tuning the interfacial couplings. However, these are still open challenges.

Very recently, silicene was successfully synthesized on Ag(111) [17,18] and ZrB_2 [19]. Buckled silicene grown on ZrB_2 thin films has an energy gap at E_F [19], suggesting the broken symmetry. On Ag(111), silicene forms a stable 4×4 superstructure. Hereafter, we call this phase 4×4 silicene. Since the 4×4 silicene takes an irregularly buckled structure, as determined by scanning tunneling microscopy (STM) and DFT calculations [17,18], the symmetry would appear to be broken. In spite of this expectation, the angle-resolved photoelectron spectroscopy (ARPES) experiments of the 4×4 silicene showed a linear band dispersion, which was thought to be a signature of the Dirac fermions [18]. However, observing part of the linear band dispersion is not always sufficient as direct proof of the Dirac fermion, because part of a parabolic band can be well approximated as a linear band. Hence, judging from the ARPES data alone would cause errors in understanding its electronic character. The spectroscopic signatures of quantum Hall effect caused by the Landau quantization under a magnetic field provide solid evidence for the Dirac fermion [20–24]. Thus measuring the current-voltage characteristics of the 4×4 silicene on Ag(111) under a magnetic field clarifies this puzzling contradiction. An analysis of electronic characteristics would clearly reveal how severely the symmetry breaking induced by the interfacial coupling with the substrate affects the electronic structure of the HC lattice. In this Letter, we present experimental evidence showing that the 4×4 silicene is neither a Dirac fermion system nor a 2D electronic system, which is reinforced by the DFT calculations.

Experiments were carried out in an ultra high-vacuum chamber with a base pressure of 5×10^{-11} Torr. The Ag (111) substrate was cleaned via several cycles of Ar^+ sputtering and annealing at 870 K. Si was *in situ* deposited by directly heating a small piece of Si wafer at a rate of 0.03 ML/min (1 ML $= 1 \times 10^{15}$ atoms cm^{-2}), which was determined from the area covered with Si. The Ag(111) substrate was kept at various temperatures below 550 K during the deposition. All the STM and scanning tunneling spectroscopy (STS) measurements were

performed at 6 K. The ac modulation of $V_{\mathrm{rms}} = 4$ mV at 400–1500 Hz was added to the sample bias voltage for the STS measurements. The DFT calculations were made by the plane-wave based Vienna *ab initio* simulation package [25,26] with projected augmented wave potentials within the generalized gradient approximation method [27]. The exchange-correlation functional of Perdew-Burke-Ernzerhof was used [28]. Details in the calculations are in the Supplemental Material [29].

Figure 1(a) shows an STM topographic image of the 4×4 silicene synthesized on Ag(111) where the STS measurements were performed. Figure 1(b) shows a magnified STM image where six protrusions are observed inside the unit cell. This feature agrees well with the 4×4 silicene structure model optimized by the DFT calculations as shown in Fig. 2(c). Six Si atoms are displaced vertically, resulting in the six protrusions in the STM image. This structure model also reproduces well the STM image as reported previously [17,18]. We measured the spectra at various positions inside the 4×4 unit cell (the white rhombus in the inset), and found the overall spectral shapes are basically the same. A V-shaped dip appears near E_F in the 4×4 silicene spectra as shown in Fig. 1(c). This feature usually shows the density of states coming from the Dirac cone structure, which was demonstrated for graphene on graphite [20,21]. However, the V-shaped dip in the STS spectrum is not a credible evidence of the Dirac fermion. As described below, 4×4 silicene on Ag(111) does not acquire the Dirac fermion.

Measuring the Landau levels (LLs) by using STS is the most direct way to judge whether the sample acquires the Dirac fermion. The cyclotron frequency (ω_C) of the Dirac fermion is given by $\omega_C = \sqrt{2}\frac{v_F}{\ell}$, where v_F is the Fermi velocity, and ℓ is the magnetic length ($\ell = \sqrt{\hbar/eB_z}$) [13]. On the Dirac fermion system, the nth LL appears at $E_n = \hbar\omega_C\sqrt{n}$ instead of conventional linear relationship. When we assume $B = 7$ T and $v_F = 10^6$ m/s, which is expected value for the freestanding silicene [10], E_n is calculated to be $95\sqrt{n}$ meV. At least low n, these levels should be clearly distinguished from the other n in our experimental setup.

Figures 1(c) and 1(d) show the evolution of the STS spectra taken for the 4×4 silicene and highly-oriented pyrolytic graphite (HOPG) with an increase in the magnetic field perpendicular to the sample, B_z. From $B_z = 0$ to 7 T, the spectrum of the 4×4 silicene does not change essentially, and characteristic structures attributed to the Landau quantization are not found. Even in the wide range (-0.5 to $+0.5$ V) spectra, no significant change can be found [29]. In contrast, LLs appear in the HOPG, and their energy positions shift with B_z. The spectral evolution of the HOPG is reasonably rationalized by a combination of massless and massive Dirac fermions [20–24]. The peaks marked with triangles and circles originate from the LLs of massless and massive Dirac fermions, respectively.

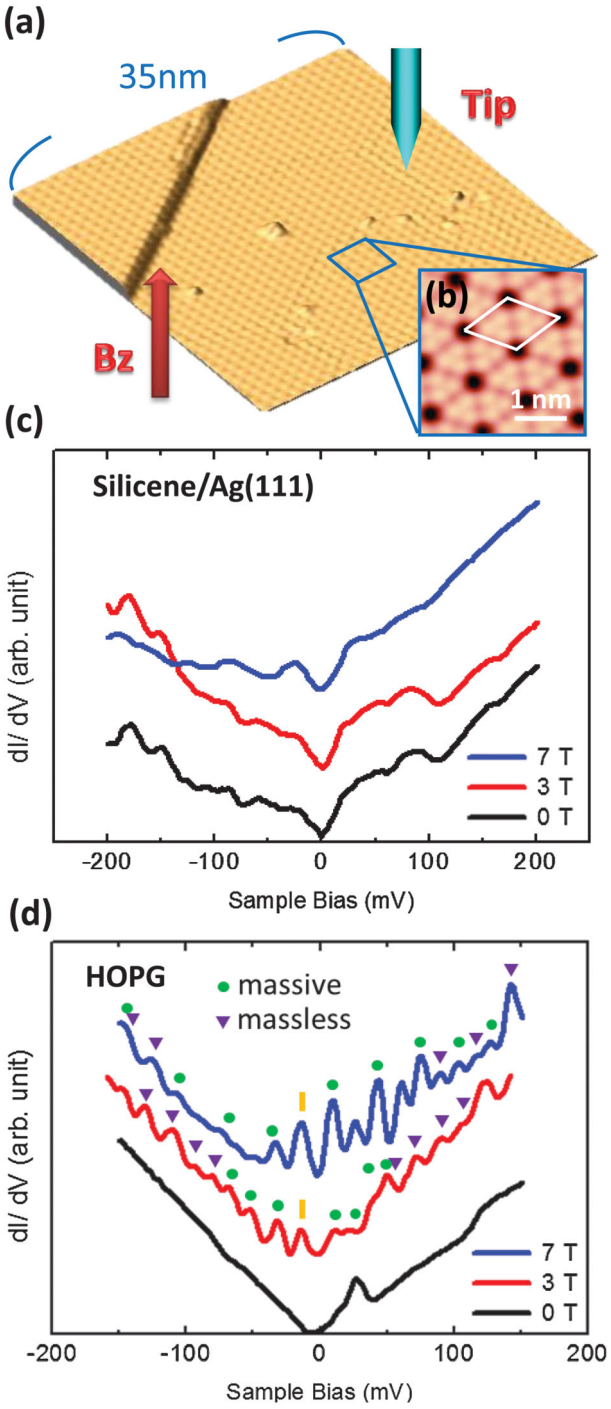

FIG. 1 (color). (a) STM image of large area of silicene (sample bias voltage $V_s = -0.70$ V and tunneling current $I_t = 0.19$ nA. The image size is 35×35 nm^2.) (b) High resolution STM image of the 4×4 silicene ($V_S = +0.50$ V and $I_t = 0.30$ nA, 3.65×3.65 nm^2). The unit cell is shown by the white rhombus. (c) The STS spectra of silicene for various magnetic fields perpendicular to the sample surface, B_z. (d) The STS spectra of HOPG for various B_Z. The purple triangles and green circles show the peaks originating from the LLs of massless and massive Dirac fermions, respectively. The $n = 0$ LL is marked by the yellow bar and the $n = 1$ LL of massive Dirac fermions is not clearly resolved in 3 T due to low magnetic field.

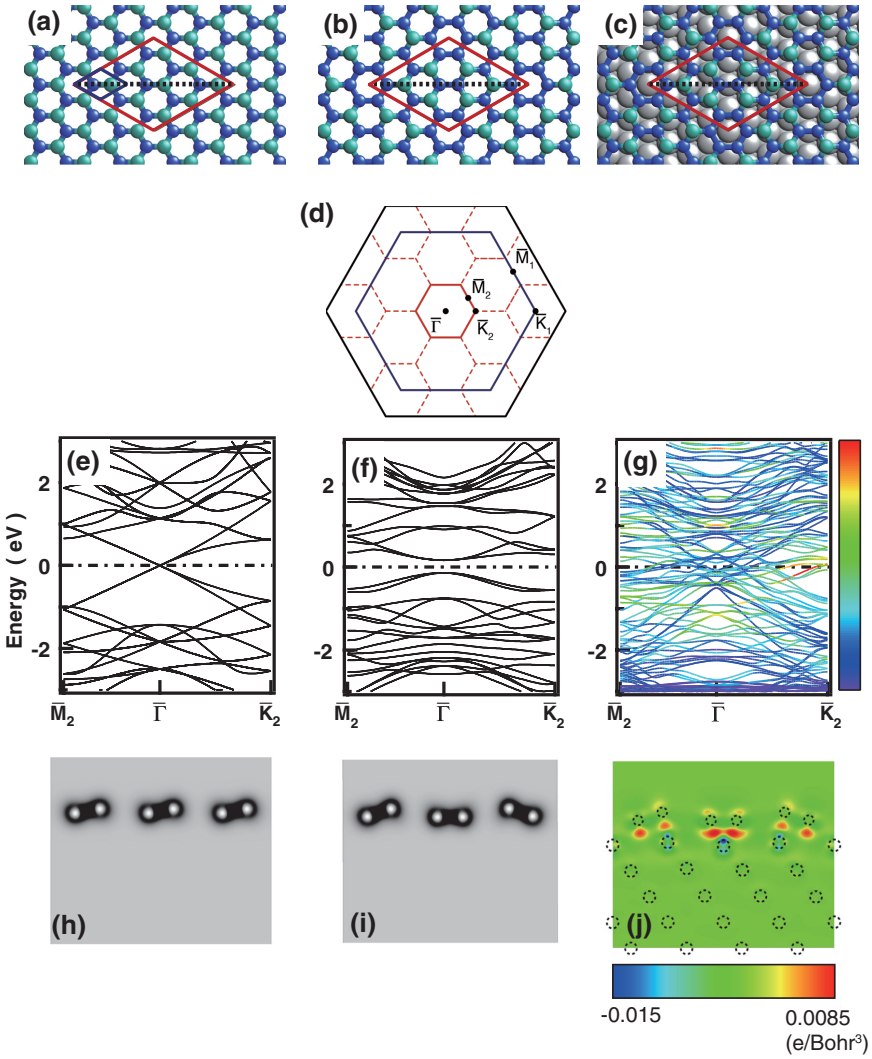

FIG. 2 (color). (a), (b), and (c) show the geometric structures of the freestanding lightly-buckled silicene (FLBS), the freestanding distorted silicene (FDS) and the 4×4 silicene, respectively. (d) Brillouin zones (BZ) corresponding to the unit cells drawn by the larger red and smaller blue rhombuses in (a) through (c). The red (blue) hexagon represents the BZ for the red (blue) rhombus drawn in (a) through (c). The black hexagon indicates the BZ of the 1×1 unit cell of Ag(111). (e), (f) and (g) show the band structures of FLBS, FDS and 4×4 silicene, respectively. The $\bar{K}_1$ point of the blue BZ is matched with the $\bar{\Gamma}$ point of the red BZ in the extended zone scheme, and thus the Dirac cone of FLBS appears at the $\bar{\Gamma}$ point. The color bar in (g) shows the relative contribution of Si $3p_z$ orbital for each band. The red (blue) shows a higher (lower) contribution. The blue bands are basically derived from the substrate Ag. The cross sections of the total charge distribution along the black dotted line in (a) and (b) are shown for (h) FLBS and (i) FDS. The black (gray) region represents a higher (lower) electron density. The cross section of the differential charge distribution (DCD) is shown for (j) the 4×4 silicene. The black dotted circles represent Si and Ag atoms. The region where the electron density increases (decreases) is colored red (blue). The figures (e)–(j) are rendered by VESTA [33].

The $n = 0$ LL marked by the yellow bar is independent of magnetic field. Note that $n = 1$ LL of massive Dirac fermions is not clearly resolved at 3 T due to the low magnetic field. Thus, we conclude that the electrons in the 4×4 silicene lose both their two dimensionality and linear dispersion that are requisite for the Dirac fermion.

The size effects might affect the magnetic field evolution of the spectra. When the domain size of silicene is small, the electrons are confined by the potential to form discrete states. The potential generated by B_z competes with this confined potential such that the LLs are not observed if the confined potential is stronger than that generated by B_z. A measure of which potential is more dominant is determined by ℓ. Since $\ell = 14.8$ and 9.7 nm for $B_z = 3$ and 7 T, respectively, and the domain size of the 4×4 silicene measured here is more than 35×35 nm^2 shown in Fig. 1(a), the size effect therefore can be ruled out while considering the absence of the LLs. Although the structural inhomogeneity and imperfections of HC lattice might also prevent the cyclotron motion of Dirac fermions and

consequently the appearance of LLs, the 4×4 silicene surface we observed is homogeneous and contains only few impurities and no domain boundary, and thus this concern can also be ruled out.

The DFT calculations reasonably explain the absence of the LLs in the 4×4 silicene on Ag(111). Figure 2 demonstrates the evolution of the band structure from freestanding lightly-buckled silicene (FLBS), freestanding distorted silicene (FDS) to the 4×4 silicene. To compare the band structure of FLBS with those of FDS and the 4×4 silicene in the same size of Brillouin zone as shown in Fig. 2(d), the structure of FLBS was optimized under the condition that the size of the unit cell [the red rhombus in Fig. 2(a)] is kept the same as that of the unit cell of the 4×4 silicene on Ag(111). The total energy, geometry and band structure calculated are not essentially different from those calculated without any constraint. The structure of the 4×4 silicene is fully optimized. The structure of FDS is the same as that of the 4×4 silicene except that the substrate is removed to distill the effect of the structure distortion on the band structure. We also considered van der Waals (vdW) interactions between silicene and Ag(111), because the vdW interactions are important for understanding graphene on metal substrates [30]. The calculated results without the vdW interactions are basically the same as those calculated by including the vdW interactions [29]. Thus, Fig. 2 shows the results calculated without the vdW interactions.

The Dirac cone appears clearly as a linear dispersion crossing at E_F for FLBS [Fig. 2(e)]. Distorting the lattice opens an energy gap at E_F for FDS [Fig. 2(f)]. The equivalence of the two sublattices inside the HC lattice disappears because of the irregularly buckled configuration of Si atoms as shown in Fig. 2(b). While the band gap opens for FDS, the overall band structure still remains similar to that of FLBS. Included the Ag substrate, the band structure drastically changes [Fig. 2(g)] (See also the magnified version of Fig. 2(g) in the Supplemental Material [29]). Although the band structure of the 4×4 silicene is very complicated, one would see neither linear dispersion nor other features observed in both FLBS and FDS band structures. Definitively, electronic bands lie around the Fermi level, but they are not derived from the Si $3p_z$ orbitals. On the contrary, the bands derived from the Si $3p_z$ orbitals seem to be located below and above 1 eV from the Fermi level. Hence, the electronic states associated with Si are strongly hybridized with the substrate states. As a result, wave functions derived from the Si $3p_z$ orbitals are delocalized into the substrate. This reasonably explains the absence of LLs in the STS experiments.

The charge distribution demonstrates clearly the interfacial coupling between the silicene and Ag substrate as shown in Figs. 2(h)–2(j). For FLBS and FDS, the charges are distributed in between neighboring Si atoms [Figs. 2(h) and 2(i)], indicating the formation of Si-Si bonding. In contrast, the charge redistribution for the 4×4 silicene is observed at the interface of the silicene and Ag clearly shown in the differential charge distribution (DCD) [Fig. 2(j)]. DCD is defined as the charge distribution calculated by subtracting the charge distributions of both isolated Ag substrate and FDS from that of the 4×4 silicene. The electron transfer takes place from Ag to Si and the bonding charges are accumulated in between the Si and the Ag atoms underneath [Fig. 2(j)]. These results indicate that the strong coupling accompanied by the charge transfer breaks the symmetry to modulate the band structure of silicene on Ag(111).

Before closing the discussion, we note that there is a discrepancy between our results and those of Vogt *et al.* who investigated the 4×4 silicene on Ag(111) using ARPES [18]. They found that a linearly dispersed band extends toward the $\bar{K}_1$ point, which appears to terminate at approximately 0.3 eV below E_F. These aspects may constitute a strong evidence for the Dirac fermion feature of the 4×4 silicene on Ag(111), and it may appear that our calculations do not successfully reproduce the electronic band structure. However, we believe there is a strong possibility that the linear band originates from the Ag bulk sp-band along the Γ-K direction. Recall that the Γ-K direction in the bulk Brillouin zone is parallel to the $\bar{\Gamma}$-$\bar{K}$ direction in the surface Brillouin zone. The radius of the Fermi surface along the Γ -K of the bulk Ag is $\sim$1.15 Å^{-1}, which implies that the Fermi surface is close to the $\bar{K}_1$ point. Our bulk band calculation yields $v_F = 1.4 \times 10^6$ ms^{-1} at the Fermi wave vector for the sp-band along the Γ-K direction, which is almost identical to the "Fermi velocity of silicene on Ag(111)" deduced by Vogt *et al.* [18]. The linear band resembles the sp-band very closely. Indeed, one would see that this band does not terminate at 0.3 eV below E_F but extends to E_F by inspecting their ARPES data in the literature. Vogt *et al.* claimed that the linear dispersion is intrinsic to the silicene because it is observed only when the Ag(111) surface is covered with silicene. However, this also can be rationalized by the final effect in photo excitation process. As Si deposition likely modifies the electronic structure above E_F, the cross section of the excitation can be enhanced so that the sp-band becomes observable. Moreover the linear band extending to $\sim$3 eV below E_F supports our idea that it is not an intrinsic band of silicene but instead the Ag sp band. Even in the calculations for freestanding silicene, the linear band dispersion does not cover such a wide energy range. Thus, we are skeptical of the Dirac fermion signature provided by Ref. [18].

Last, we note here that the other phases of silicene on Ag(111) [31,32] were not suitable for measuring LLs. As described above, the homogeneity and sufficiently large area of the silicene sheet are required to observe LLs. However, other phases of silicene on Ag(111) except the 4×4 usually appear in mixed phase and the domain of any

single phase is not large enough to rule out the size effect. We occasionally succeeded in synthesizing a relatively large area of the $\sqrt{13} \times \sqrt{13}R13.9°$ phase of silicene on Ag(111). In the STS spectra of the $\sqrt{13} \times \sqrt{13}R13.9°$ (not shown here), no peak structure appeared and the spectra unchanged essentially up to $B_z = 6$ T.

To summarize, we have investigated the electronic structure of 4×4 silicene on Ag(111) by STS and DFT calculations. Our results show that the electronic structure of silicene is modified significantly by the symmetry breaking through the interfacial coupling with Ag(111). As a result, LLs are not observed and thus the charge carriers inside silicene become non-Dirac fermions. The electrons of the π and π^* bands are delocalized into the substrate through the hybridization, implying that the 4×4 silicene can no longer be a 2D electronic system. To realize the exotic properties of silicene predicted theoretically [10,15,16], it is prerequisite to find a substrate that avoids undesirable symmetry breaking to silicene.

This was supported by Grants-in-Aid for Scientific Research (No. 24241040) from the Ministry of Education, Culture, Sports, Science and Technology, Japan (MEXT), World Premier International Research Center Initiative (WPI), MEXT, and the National Science Council (No. 100-2917-I-564-022), Taiwan. The computation was done using the facilities of the Supercomputer Center, the Institute for Solid State Physics, The University of Tokyo, and the RIKEN Integrated Cluster of Clusters (RICC) facility.

*n-takagi@k.u-tokyo.ac.jp

[1] K. S. Novoselov, A. K. Geim, S. V. Morozov, D. Jiang, Y. Zhang, S. V. Dubonos, I. V. Grigorieva, and A. A. Firsov, Science **306**, 666 (2004).
[2] J. Nagamatsu, N. Nakagawa, T. Muranaka, Y. Zenitani, and J. Akimitsu, Nature (London) **410**, 63 (2001).
[3] N. Tajima, S. Sugawara, R. Kato, Y. Nishio, and K. Kajita, Phys. Rev. Lett. **102**, 176403 (2009).
[4] Y. Kubota, K. Watanabe, O. Tsuda, and T. Taniguchi, Science **317**, 932 (2007).
[5] B. Radisavljevic, A. Radenovic, J. Brivio, V. Giacometti, and A. Kis, Nat. Nanotechnol. **6**, 147 (2011).
[6] D. Xiao, W. Zhu, Y. Ran, N. Nagaosa, and S. Okamoto, Nat. Commun. **2**, 596 (2011).
[7] K. Takeda and K. Shiraishi, Phys. Rev. B **50**, 14916 (1994).
[8] G. G. Guzmán-Verri and L. C. Lew Yan Voon, Phys. Rev. B **76**, 075131 (2007).
[9] S. Cahangirov, M. Topsakal, E. Aktrük, H. Sahin, and S. Ciraci, Phys. Rev. Lett. **102**, 236804 (2009).
[10] C.-C. Liu, W. Feng, and Y. Yao, Phys. Rev. Lett. **107**, 076802 (2011).
[11] A. Kara, H. Enriquez, A. P. Seitsonen, L. C. Lew Yan Voon, S. Vizzini, B. Aufray, and H. Oughaddou, Surf. Sci. Rep. **67**, 1 (2012).
[12] M. I. Katsnelson, K. S. Novoselov, and A. K. Geim, Nat. Phys. **2**, 620 (2006).
[13] A. H. Castro Neto, F. Guinea, N. M. R. Peres, K. S. Novoselov, and A. K. Geim, Rev. Mod. Phys. **81**, 109 (2009).
[14] A. S. Mayorov, D. C. Elias, M. Mucha-Kruczynski, R. V. Gorbachev, T. Tudorovskiy, A. Zhukov, S. V. Morozov, M. I. Katsnelson, V. I. Fal'ko, A. K. Geim, and K. S. Novoselov, Science **333**, 860 (2011).
[15] N. D. Drummond, V. Zólyomi, and V. I. Fal'ko, Phys. Rev. B **85**, 075423 (2012).
[16] M. Ezawa, Phys. Rev. Lett. **109**, 055502 (2012).
[17] C. L. Lin, R. Arafune, K. Kawahara, N. Tsukahara, E. Minamitani, Y. Kim, N. Takagi, and M. Kawai, Appl. Phys. Express **5**, 045802 (2012).
[18] P. Vogt, P. D. Padova, C. Quaresima, J. Avila, E. Frantzeskakis, M. C. Asensio, A. Resta, B. Ealet, and G. L. Lay, Phys. Rev. Lett. **108**, 155501 (2012).
[19] A. Fleurence, R. Friedlein, T. Ozaki, H. Kawai, Y. Wang, and Y. Yamada-Takamura, Phys. Rev. Lett. **108**, 245501 (2012).
[20] T. Matsui, H. Kambara, Y. Niimi, K. Tagami, M. Tsukada, and H. Fukuyama, Phys. Rev. Lett. **94**, 226403 (2005).
[21] Y. Niimi, H. Kambara, T. Matsui, D. Yoshioka, and H. Fukuyama, Phys. Rev. Lett. **97**, 236804 (2006).
[22] G. Li and E. Y. Andrei, Nat. Phys. **3**, 623 (2007).
[23] D. L. Miller, K. D. Kubista, G. M. Rutter, M. Ruan, W. A. de Heer, P. N. First, and J. A. Stroscio, Science **324**, 924 (2009).
[24] G. Li, A. Luican, and E. Y. Andrei, Phys. Rev. Lett. **102**, 176804 (2009).
[25] G. Kresse and J. Furthmüller, Phys. Rev. B **54**, 11169 (1996).
[26] G. Kresse and J. Furthmüller, Comput. Mater. Sci. **6**, 15 (1996).
[27] P. E. Blöchl, Phys. Rev. B **50**, 17953 (1994).
[28] J. P. Perdew, K. Burke, and M. Ernzerhof, Phys. Rev. Lett. **77**, 3865 (1996).
[29] See Supplemental Material at http://link.aps.org/supplemental/10.1103/PhysRevLett.110.076801 for supplementary texts and figures.
[30] M. Vanin, J. J. Mortensen, A. K. Kelkkanen, J. M. Garcia-Lastra, K. S. Thygesen, and K. W. Jacobsen, Phys. Rev. B **81**, 081408 (2010).
[31] H. Jamgotchian, Y. Colignon, N. Hamzaoui, B. Ealet, J. Y. Hoarau, B. Aufray, and J. P. Bibérian, J. Phys. Condens. Matter **24**, 172001 (2012).
[32] R. Arafune, C. L. Lin, K. Kawahara, N. Tsukahara, E. Minamitani, Y. Kim, N. Takagi, and M. Kawai, Surf. Sci. **608**, 297 (2013).
[33] K. Momma and F. Izumi, J. Appl. Crystallogr. **41**, 653 (2008).